Depolarization shift of the intersubband resonance in a quantum well with an electron-hole plasma

I. Shtrichman,[1,2] C. Metzner,[2] E. Ehrenfreund,[1] D. Gershoni,[1] K. D. Maranowski,[2] and A. C. Gossard[2]
[1]*Physics Department and Solid State Institute, Technion-Israel Institute of Technology, Haifa 32000, Israel*
[2]*Materials Department, University of California, Santa Barbara, California 93106*
(Received 7 July 2001; published 14 December 2001)

We study the depolarization shift of the electronic intersubband resonance at various electron-hole plasma densities. Using a time-resolved interband-pump–intersubband-probe technique, we measure the intersubband transitions in GaAs quantum wells. The pump pulse generates an electron-hole plasma, which then gradually decays by radiative recombination, while the probe pulse monitors the conduction band intersubband absorption spectrum as a function of the momentary plasma density. The measured time/density-dependent shift of the intersubband resonance energy is quantitatively explained by a density functional model accounting for the static and dynamic many-body effects in the electron-hole plasma. It turns out that the holes play an important role in minimizing the static Hartree potential. Their presence, however, does not significantly affect the measured dynamic depolarization shift of the electronic intersubband resonance.

DOI: 10.1103/PhysRevB.65.035310 PACS number(s): 73.21.Fg, 78.47.+p, 71.10.−w

I. INTRODUCTION

Intersubband (ISB) transitions in semiconductor quantum wells (QW's) span the electromagnetic spectrum from the far-infrared region[1] to the near-infrared region[2] and thus have important technological implementations. Due to their large oscillator strength and the ability to control the transition energy by changing the structural parameters of the QW, intersubband transitions have been successfully implemented in optoelectronic devices such as infrared (IR) photodetectors[3] and lasers.[4,5]

Extensive research efforts have been devoted to theoretical and experimental studies of these optical transitions in the presence of either dense electron plasma or hole plasma.[6] It has been shown both theoretically and experimentally that the many-electron interaction changes the single-electron intersubband resonant transition energy and its spectral shape.[7] This effect, known as the ''depolarization shift,'' was only studied for a one-component electron plasma. In this work we report on experimental measurements of the depolarization shift as a function of the density of a two-component electron-hole (e-h) plasma. Our measurements are quantitatively compared with a theoretical, density-functional model that accounts for the many-body effects of the e-h plasma.

The energy separation between the lowest subbands of an empty QW, $\epsilon_{21}(0)=\epsilon_2(0)-\epsilon_1(0)$, is fixed by the material structure along the growth direction, z. In a QW with finite two-dimensional (2D) carrier density n, the actual photon energy $E_{\rm res}(n)$ of the resonance peak in an ISB absorption experiment is different from $\epsilon_{21}(0)$ due to many-body effects. The total observed energy shift can be decomposed into static (equilibrium) and dynamic (resulting from the ac electric field of the incident light) many-body corrections:[7] $\Delta E_{\rm tot}(n)=\Delta E_{\rm sta}(n)+\Delta E_{\rm dyn}(n)$.

The static contribution $\Delta E_{\rm sta}(n)=\epsilon_{21}(n)-\epsilon_{21}(0)$ consists of the Hartree term (H) and its exchange-correlation corrections (XC). In the framework of the density functional theory, these effects can be accounted for by a self-consistent solution of Schroedinger's equation, Poisson's equation, and the local exchange-correlation potential.

The dynamic contribution $\Delta E_{\rm dyn}(n)=E_{\rm res}(n)-\epsilon_{21}(n)$ consists of the depolarization shift (D) and the excitonic correction (exc). These effects are due to the spatial-temporal three-dimensional density oscillations $\Delta n^{(3)}(z,t)$ of the electron plasma, driven by the external ir light field. The density fluctuations are connected with an induced dynamic Coulomb potential, which is acting on each electron as a perturbation. In formal analogy to the static case, the dynamic potential can be decomposed into direct part (causing the depolarization shift) and its exchange-correlation corrections (responsible for the so-called excitonic shift).

All four terms mentioned above have their characteristic sign and carrier density dependence, and are generally of the same order of magnitude (few meV in most realistic cases). In order to understand the many-body physics of intersubband absorption, it is therefore essential to vary and control the density of the plasma in the system.

In the past, various methods have been employed in order to tune the carrier density in the QW(s). In most cases a series of samples were grown with different doping levels in the well[8] or with different spacer thickness between the doped layer and the well (modulation doping).[9–11] Other techniques to control n used a continuous depletion of a modulation doped QW by an electric field[12] or by a hydrostatic pressure.[13]

In this work we present an all-optical approach, in which electron-hole pairs are generated by interband excitation (visible light), while the electronic intersubband absorption is simultaneously monitored by infrared light. This technique has few advantages over the previously used schemes.

Most important, it allows a continuous variation of the electron-hole density over a relatively wide range. In principle, this tunability can be achieved even with continuous-wave (CW) excitation, simply by changing the power of the pump laser. An alternative way, implemented in this work, is a time-resolved measurement. A high density of electron-hole pairs $n(0)$ is initially created by an intense and short pump pulse. The excited carriers then thermalize quickly (picoseconds) into their respective quasiequilibrium, and subsequently, on a much longer time scale (nanosecond), decay

via radiative recombination, with $n(t)$ gradually dropping to zero. At each instant the carriers quasi-Fermi-distributions adjust adiabatically to the plasma density, and by probing the conduction-band ISB absorption at different delay times with respect to the pump pulse, we effectively obtain the ISB spectrum as a function of n. While in a CW experiment the carriers energy distributions are constantly perturbed by the intense pump laser, which may also cause artifacts due to power-dependent heating of the sample, such effects are minimized in the time-resolved approach.

Another interesting feature of the optical carrier generation is the approximate local charge neutrality of the QW, such that the self-consistent band bending is small and nearly independent of $n(t)$. This stands in contrast to most of the other density tuning methods, where the Hartree term often dominates the evolution of the ISB absorption spectrum with electron density.

Furthermore, in the case of electron-hole plasma, the ISB absorption can be affected by *dynamic* interband coupling (electron-hole depolarization shift) or by *microscopic* electron-hole interactions (interband excitonic effects). While, as we will show, for our specific sample parameters the holes have a negligible influence on the electronic ISB resonance, interesting physical phenomena are expected in the strong coupling regime.

The paper is organized as follows: In Sec. II we introduce our theoretical model. In Sec. III we briefly display the sample and the experiment setup. In Sec. IV we show our experimental results and compare them to the theory. Finally, we conclude in Sec. V.

II. THEORY

A. Static band-structure model

Since in our experimental multi-QW structure the coupling between neighboring wells is negligible, we focus on a single QW of width a. In a first step, we compute the self-consistent static band-structure of the QW, considering only electrons (e) and heavy holes (h) of equal densities $n=p$. Mixing effects of light- and heavy-hole states are ignored; however, we account for nonparabolicity of the conduction-band dispersion by an energy-dependent effective mass $m=m(E)$.[14] In the following we often skip the electron and hole indices, e and h, for reasons of clarity. We also define in advance the Coulomb coupling constant $K_0=e^2/(4\pi\epsilon\epsilon_0)$.

The total effective potential $V(z)$ acting on the electrons consists of the bare QW potential $V_{\mathrm{QW}}(z)$ (in our case, a square well of width $a=5.7$ nm and height $U_e=297.8$ meV or $U_h=174.9$ meV), the direct Hartree term

$$V_H(z)=4\pi K_0\int_{-\infty}^{\infty}dz'\int_{-\infty}^{z'}dz[n^{(3)}(z)-p^{(3)}(z)], \quad (1)$$

and the standard exchange-correlation correction[7]

$$V_{\mathrm{XC}}(z)=V_{\mathrm{xc}}(n^{(3)}(z)), \quad (2)$$

where $n^{(3)}(z)$ is the local three-dimensional (3D) charge density. Analogous equations hold, of course, for the holes.

These equations are solved self-consistently with the Schrödinger equation, yielding the subband levels ϵ_i and corresponding wave functions $\varphi_i(z)$ for a given 2D electron-hole plasma density n. We repeat the above local density approximation calculation for a range of densities and thereby compute the renormalized electronic ISB separation $\epsilon_{21}(n)=\epsilon_2(n)-\epsilon_1(n)$ as a function of n.

B. Static electron-hole interactions beyond the Hartree approximation

We note that the theory above accounts for the direct Coulomb interactions between electrons and holes, but neglects interband exchange processes (related to the Pauli exclusion principle) and electron-hole correlations (for example, excitonic binding effects). Interband exchange is known to be small in most systems. On the other hand, the formation of bound electron-hole pairs is a strong effect in the low-density regime, which gradually disappears with increasing plasma density due to efficient screening. From the viewpoint of the electrons, such correlations result in a further lowering of their energy levels, in addition to the Hartree attraction by the mean hole density distribution. The binding energy E_{ij}^{bind} of an exciton, with the electron in subband i and the hole in subband j, provides an estimate for this effect. However, the quantity relevant for the ISB peak shift is the *difference* $E_{21}^{\mathrm{bind}}-E_{11}^{\mathrm{bind}}$, which is expected to be smaller and more weakly density dependent. Although excitonic effects may not be altogether negligible, we choose to ignore them in our present model.

C. Dynamic electron-electron interactions

Next, using the self-consistent wave functions and subband energy levels from above, we calculate the dynamic electron-electron corrections to the ISB absorption spectrum, using the standard time-dependent random phase approximation. According to this theory,[7] the electronic ISB resonance occurs at photon energy

$$E_{\mathrm{res}}(n)=\epsilon_{21}(n)\sqrt{1+\alpha(n)-\beta(n)}, \quad (3)$$

with

$$\alpha(n)=2T_{ee}n/\epsilon_{21}(n) \quad (4)$$

and

$$\beta(n)=\frac{-2n}{\epsilon_{21}(n)}\int dz[\varphi_1(z)]^2[\varphi_2(z)]^2\frac{\delta V_{\mathrm{xc}}(n^{(3)})}{\delta n^{(3)}}(z). \quad (5)$$

The ISB Coulomb integral T_{ee} for laterally homogeneous systems can be written as

$$T_{ee}=-2\pi K_0\int dz\int dz'\varphi_2(z)\varphi_1(z)\times|z-z'|\varphi_2(z')\varphi_1(z'). \quad (6)$$

The two dimensionless parameters α and β control the depolarization shift of the ISB resonance and its excitonic correction, respectively.

D. Dynamic electron-hole interactions

Finally, we have to discuss the possibility of dynamic (light induced) interactions between electrons and holes. Again, we divide these coupling effects into Hartree-like (depolarization) and exchange-correlation (excitonic) contributions. Not having accounted for the static interband exchange-correlation processes, we will also neglect their dynamic counterpart in this paper. In order to build a model for the interband depolarization effect, it is useful to first rederive Eq. (3) in a slightly simpler approximation.

1. Linear electronic depolarization shift

In most practical cases, the parameter $\alpha(n)$ is small compared to unity, so that it is sufficient to linearize Eq. (3). If we set $\beta(n)=0$ for the time being, we can write the linearly depolarization shifted ISB resonance energy as

$$E_{\mathrm{lin}}(n)=\epsilon_{21}(n)+nT_{ee}\,. \tag{7}$$

If we were dealing with holes instead of electrons, we could define:

$$H_{\mathrm{lin}}(n)=\eta_{21}(n)+pT_{hh}\,, \tag{8}$$

where $\eta_{21}(n)$ is the self-consistent subband separation between the ground and first excited hole subbands and T_{hh} is calculated analogously to Eq. (6).

The linear result, Eq. (7) is easily derived for a system containing only electrons by solving the frequency-dependent, dynamic equation of the Coulomb-interacting particles. The dimensionless oscillation amplitude $A_e(\omega)$ of the plasma is determined by the total time-dependent potential W_{tot} acting on the electrons times their response function $P_e(\omega)$:[15]

$$A_e(\omega)=W_{\mathrm{tot}}P_e(\omega)=\frac{W_{\mathrm{tot}}}{\epsilon_{21}^{(el)}(n)-\hbar\omega-i\Gamma_e}, \tag{9}$$

where Γ is a phenomenological damping constant. The total potential consists of the external and the induced parts:

$$W_{\mathrm{tot}}=(\mu_eF/2)-nT_{ee}A_e(\omega), \tag{10}$$

where $\mu_e=<2|ez|1>$ is the dipole moment of the intersubband transition and F the electric field strength of the incident light. Inserting Eq. (10) into Eq. (9) gives a dynamic equation, which can be solved for $A(\omega)$, yielding

$$A_e(\omega)=\frac{\mu_eF/2}{P_e^{-1}(\omega)+nT_{ee}}=\frac{\mu_eF/2}{[\epsilon_{21}(n)+nT_{ee}]-\hbar\omega-i\Gamma}. \tag{11}$$

The resonance frequency of the interacting electron plasma is determined by the (damped) pole of the above expression, i.e., it occurs at the photon energy E_{lin} of Eq. (7).

2. Linear electron-hole depolarization shift

It is now straightforward to extend this theory to the case of an interacting electron-hole system. We then have to consider two coupled equations for the oscillation amplitudes $A_e(\omega)$ and $A_h(\omega)$ of the two types of particles:

$$A_e(\omega)=P_e(\omega)[\mu_eF/2-nT_{ee}A_e(\omega)-pT_{eh}A_h(\omega)],$$
$$A_h(\omega)=P_h(\omega)[\mu_hF/2-pT_{hh}A_h(\omega)-nT_{eh}A_e(\omega)]. \tag{12}$$

Solving this system for $A_e(\omega)$ yields

$$A_e(\omega)=\frac{(\mu_eF/2)-B(\omega)(\mu_hF/2)}{[E_{\mathrm{lin}}(n)-B(\omega)nT_{eh}]-\hbar\omega-i\Gamma_e}, \tag{13}$$

where we have used the abbreviation

$$B(\omega)=\frac{pT_{eh}}{H_{\mathrm{lin}}(p)-\hbar\omega-i\Gamma_h}. \tag{14}$$

Again we analyze the poles of Eq. (13) to find the two resonance frequencies of the coupled oscillators:

$$\hbar\omega_{1,2}=\tfrac{1}{2}[E_{\mathrm{lin}}(n)+H_{\mathrm{lin}}(p)]\pm\tfrac{1}{2}|E_{\mathrm{lin}}(n)-H_{\mathrm{lin}}(p)|\sqrt{1+\gamma}, \tag{15}$$

with the dimensionless coefficient

$$\gamma=\left(\frac{\sqrt{np}T_{eh}}{E_{\mathrm{lin}}(n)-H_{\mathrm{lin}}(p)}\right)^2. \tag{16}$$

3. Limiting cases

In the following, we briefly discuss the expected modifications to the ISB spectrum related to the linearized electron-hole depolarization effect, as described by Eq. (15). Obviously, the important parameter is the ratio between the electron-hole interaction energy $\sqrt{np}T_{eh}$ and the difference of the individually depolarization shifted resonance energies of the two particles. We can distinguish three cases.

The first limit is $\gamma=0$, which would occur if we could turn off the electron-hole interaction completely. If this were the case, the resonance positions would be $\hbar\omega_1=E_{\mathrm{lin}}(n)$ and $\hbar\omega_2=H_{\mathrm{lin}}(p)$, as in mutually independent electron and hole plasmas.

The second, practically most relevant case corresponds to small but finite γ. Then the lower-energy transition becomes slightly redshifted and the higher-energy transition blue shifted by the electron-hole interaction. For the specific parameters of our sample, we obtain even at the relatively high carrier density $n=p=10^{12}$ cm^{-2} a value of only $\gamma=1.836\times10^{-3}$, yielding $\sqrt{1+\gamma}=1.000\,917$.

Finally, in the extreme case of exactly equal resonances, $E_{\mathrm{lin}}(n)=H_{\mathrm{lin}}(p)$, one obtains

$$\hbar\omega_{\mathrm{res}}^{\mathrm{ext}}=E_{\mathrm{lin}}(n)\pm\frac{1}{2}\sqrt{np}T_{eh}\,, \tag{17}$$

i.e., the two absorption peaks do not cross each other and show a minimum splitting given by the electron-hole-interaction energy.

III. EXPERIMENT

The undoped multi-QW sample was grown by molecular beam epitaxy on a (100)-oriented semi-insulating GaAs substrate. It contains 25 periods of a nominally 6 nm thick GaAs well and 12 nm thick $Al_{0.33}Ga_{0.67}As$ barrier. The two edges of the sample were polished at 45° to the growth axis, in order to form a waveguide for the mid-ir radiation with an electric field component parallel to the growth direction. The time-resolved photoinduced intersubband absorption setup consists of a frequency-doubled mode-locked neodymium-doped yttrium aluminum garnet (Nd:YAG) laser that simultaneously pumps three picosecond dye lasers at a repetition rate of 76 MHz. The pulses from two dye lasers, each with an average power of ≈ 400 mW, are mixed in a non-linear $AgGaS_2$ crystal to produce their energy difference—a spectrally tunable ir probe pulse with an average power of ≈ 50 μW. The third dye laser produces the visible pump pulse. In order to prevent heating of the sample at high excitation densities, the pump pulse frequency was reduced by a factor of 20 using a cavity dumper. The average power of the pump pulse was changed in the range of 3 to 30 mW, and the excitation spot diameter was ≈ 100 μm.

The photoinduced changes in transmission through the ir waveguide are measured by a mercury cadmium telluride detector and a lock-in amplifier synchronized with the cavity dumper. The temporal evolution of the ISB absorption is studied by varying the delay time between the probe pulse and the pump pulse.[16,17] The setup temporal and spectral resolutions are 4 ps and 0.5 meV (both in the visible and in the ir range), respectively. The measurements were done with the sample mounted on a cold finger cryostat at 10 K. The pump pulse was spectrally tuned to the low-density first *e-h* excitonic resonance energy (1.63 eV), and the probe energy was tuned around the E_1-E_2 intersubband resonance.

IV. RESULTS AND DISCUSSION

A. Time-resolved ISB absorption spectra

We have measured the transient ISB absorption $\alpha(\omega,\Delta t)$ as a function of the delay time Δt, for various fixed probe energies $\hbar\omega$. Constant-time cross sections $\alpha(\omega,\Delta t_i)$ from the data thus obtained are presented in Fig. 1. The spectra are vertically displaced for clarity and a short horizontal line represents the zero intensity of each spectrum. The solid lines in Fig. 1 are Gaussian fits to the experimental data.

We find that the spectrum width is almost constant (FWHM$\approx$5.5 meV) and relate it to both homogeneous broadening due to the levels nonparabolicity[7] and to inhomogeneous broadening due to the large number of periods in this structure. We observe a spectral shift of the ISB absorption peak as the time evolves. It shifts slightly (≈ 1 meV) to high energies at short delay times, and starting from 60 ps it shifts gradually back to low energies (≈ -2.5 meV).

B. Integral absorption and peak position

Using the Gaussian line fits from Fig. 1, we display in Fig. 2 the spectrally integrated ISB absorption $I(\Delta t)$ (solid squares, left axis) and the energy of the absorption peak $E_{\rm res}(\Delta t)$ (open circles, right axis) as functions of the delay time. For the integral absorption we note four temporal regimes:

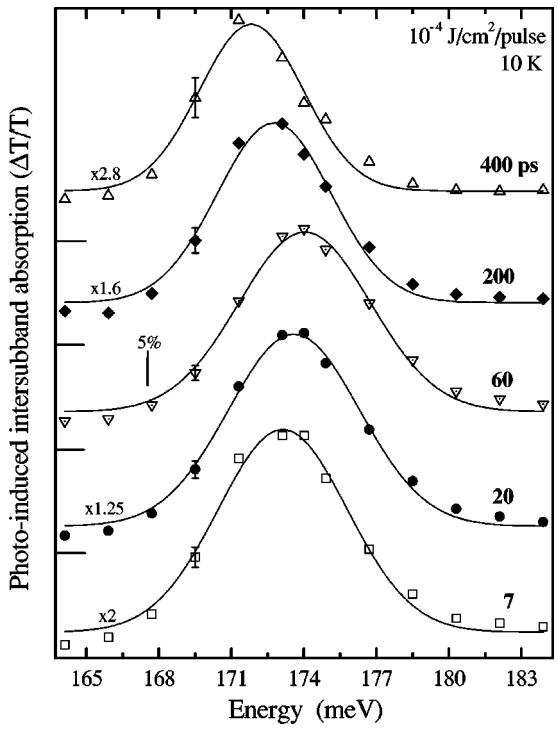

FIG. 1. The E_1-E_2 intersubband absorption spectra for various delay times between the pump and probe pulses. The excitation energy and average intensity are 1.63 eV and 30 mW, respectively. The solid lines are Gaussian fits to the data.

(a) At negative times, much earlier than the arrival of the pump pulse, the ISB absorption is zero. Starting at 30 ps before the beginning of the fast rise, the absorption rises slightly due to a small leading pulse from the cavity dumper which precedes the main pulse.

(b) At short delay time (0–7 ps), the ISB absorption rises rapidly due to the population of E_1 by the pump pulse.

(c) After the pump pulse ends, the absorption rises for few tens of picoseconds and reaches its maximum at ≈ 50 ps.

(d) Next, the ISB absorption drops over few hundreds of picoseconds due to the radiative decay of the excited carrier population.

The solid line represents a fit to the spectrally integrated absorption, using a single exponential rise time and single exponential decay time phenomenological model:

$$I(\Delta t')=[a-b\,e^{-\Delta t'/\tau_1}]e^{-\Delta t'/\tau_2}. \tag{18}$$

Here, $\Delta t'$ is the time delay relative to the end of the exciting pulse (at absolute delay time $\Delta t_0=8$ ps). From this fitting we obtain a rise time $\tau_1=20$ ps and a decay time $\tau_2=250$ ps. While the source of the rise time is not totally understood, the decay time is characteristic of GaAs QW's at this temperature.[18]

In Fig. 2, starting from the end of the pump pulse, the peak spectral position $E_{\rm res}(\Delta t)$ first blueshifts until it reaches

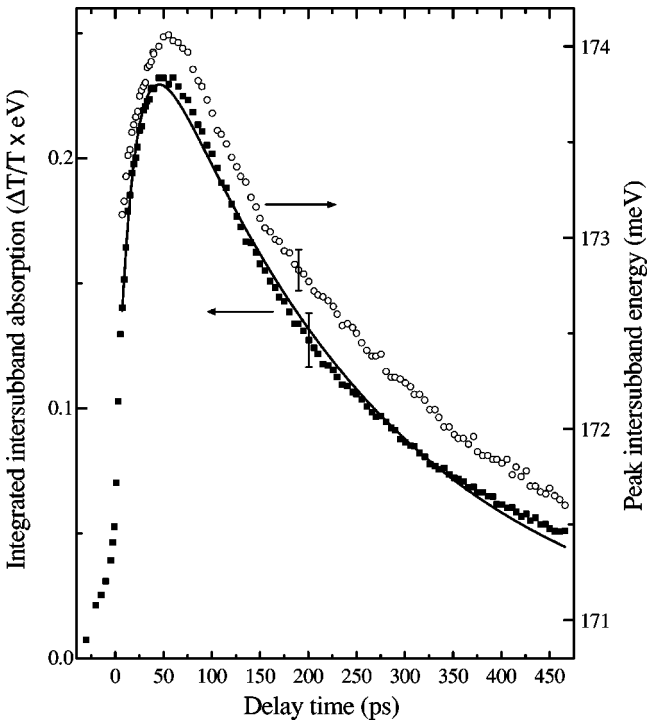

FIG. 2. The spectrally integrated intersubband absorption (solid squares, left axis) and the peak intersubband energy (open circles, right axis) as a function of delay time, attained from the Gaussian fits to the spectra of Fig. 1. The solid line is a fit to the integrated absorption of a single exponential rise–single exponential decay phenomenological model.

a maximum at ≈ 50 ps and then redshifts at longer times. From this plot it is obvious that the ISB transition energy closely follows the dynamics of the electron population in the ground subband.

C. Density dependence of the peak position

We compute the electron density $n(\Delta t)$ from the measured spectrally integrated ISB absorption $I(\Delta t)$ using an eight-band $\mathbf{k}\cdot\mathbf{p}$ model.[19] This allows us to convert the temporal function $E_{\mathrm{res}}(\Delta t)$ of Fig. 2 into a static, density-dependent function $E_{\mathrm{res}}(n)$, which is then plotted in Fig. 3. In our case, as the density varies between about $n=1\times10^{11}$ cm^{-2} and $n=4\times10^{11}$ cm^{-2}, the peak position increases from 171.6 meV to 174 meV in an almost linear way. We repeated these measurements also at a factor of 3 and factor of 10 lower excitation intensities. By comparing the ISB absorption to $\mathbf{k}\cdot\mathbf{p}$ calculations, we find that these lower intensities correspond to a factor of 1.4 and factor of 2.7 lower densities, respectively, due to the interband exciton resonance bleaching.[20] In these measurements we find behavior similar to the above with smaller energy shifts, in good agreement with the model.

D. Interpretation of the observed peak shift

The function $E_{\mathrm{res}}(n)$ can be directly compared to the theoretical model described above. In order to match the calculated energy to the experimental data we fit only the QW width a and find $a=5.7$ nm, which is one monolayer narrower than the nominal value. The resulting theoretical density dependence of the peak position, calculated using Eq. (3), is shown as a solid line in Fig. 3. The inset shows the individual contributions to the total peak shift.

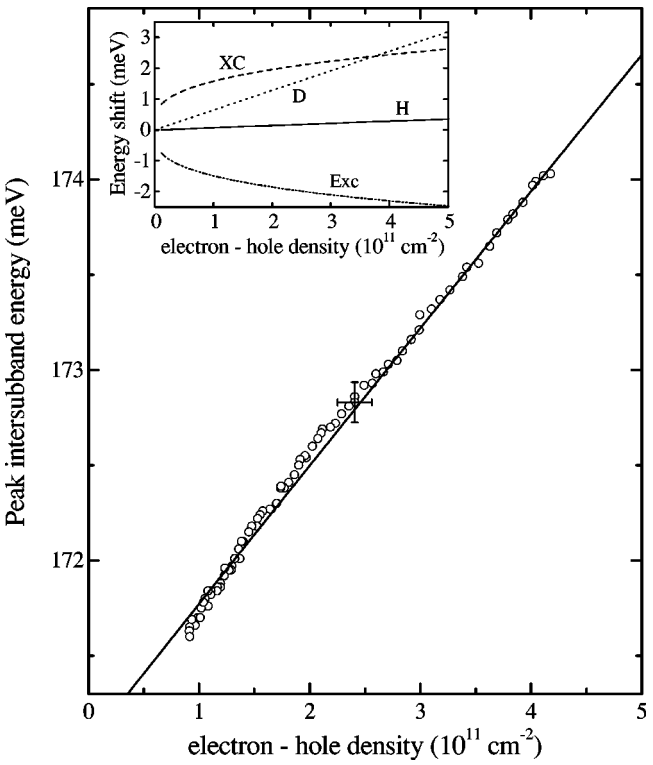

FIG. 3. The peak intersubband energy as a function of the electron-hole density. The open circles are the experimental data, extracted from Fig. 2, and the solid line is the calculated transition energy. The inset displays the individual contributions of the different terms in our model to the energy shift with respect to the bare E_1-E_2 splitting (170.9 meV). H, Hartree; XC, exchange-correlation; Exc, exciton; D, depolarization.

We note that in general the exchange-correlation shift $\Delta E_{\mathrm{XC}}\propto n^{1/3}$ and the excitonic shift $\Delta E_{\mathrm{exc}}\propto -n^{1/3}$ are roughly proportional to the cube root of the carrier density, with positive and negative prefactors, respectively. In our specific case it furthermore turns out that these two terms almost cancel each other.

In systems with only one type of carrier, the negative Hartree term $\Delta E_H\propto -n$ and the positive depolarization term $\Delta E_D\propto n$ are proportional to the carrier density. In the two-component plasma discussed here, however, the presence of holes prevents band bending as discussed in the Introduction. Therefore, the Hartree shift of the ISB resonance is slightly positive and almost negligible (solid line in the inset). These conditions lead to the rather unusual situation where the observed blueshift of the ISB peak with increasing carrier density is almost exclusively due to the depolarization effect, $\Delta E_{\mathrm{res}}(n)\approx\Delta E_D(n)$, and is therefore linear to a good approximation.[21]

V. CONCLUSION AND OUTLOOK

In conlusion, we have demonstrated an all-optical technique to measure the ISB absorption in a QW as a continu-

ous function of its 2D carrier density. The simultaneous presence of holes and electrons in this technique leads to an effective reduction of static band-bending effects, but it does not further affect the electronic ISB resonance. We were able to quantitatively describe the experimentally observed shift of the ISB peak energy as a function of the two-component plasma concentration by a density functional approximation. We have shown that interesting dynamic effects are expected for systems designed in such a way that the individual ISB resonances of the uncoupled carriers are similar and of comparable oscillator strength.

ACKNOWLEDGMENTS

The work at the Technion was supported by the Israel Science Foundation (Grant No. 335/99). One of the authors (C.M.) is greatful for the financial support by the Humboldt Foundation.

[1] K. Craig, B. Galdrikian, J.N. Heyman, A.G. Markelz, J.B. Williams, M.S. Sherwin, K. Campman, P.F. Hopkins, and A.C. Gossard, Phys. Rev. Lett. **76**, 2382 (1996).

[2] C. Gmachl, H.M. Ng, S.-N.G. Chu, A.Y. Cho, Appl. Phys. Lett. **77**, 3722 (2000).

[3] B.F. Levine, J. Appl. Phys. **74**, R1 (1993).

[4] J. Faist, F. Capasso, D.L. Sivco, C. Sirtori, A.L. Hutchinson, and A.Y. Cho, Science **264**, 553 (1994).

[5] O. Gauthier-Lafaye, F.H. Julien, S. Cabaret, J.-M. Lourtioz, G. Strasser, E. Gornik, M. Helm, and P. Bois, Appl. Phys. Lett. **74**, 1537 (1999).

[6] For recent works on intersubband transitions in QW's see R.A. Kaindl, M. Wurm, K. Reimann, M. Woerner, T. Elsaesser, C. Miesner, K. Brunner, and G. Abstreiter, Phys. Rev. Lett. **86**, 1122 (2001); L.V. Kulik, I.V. Kukushkin, V.E. Kirpichev, K.v. Klitzing, and K. Eberl, *ibid.* **86**, 1837 (2001).

[7] M. Helm, in *Intersubband Transitions in Quantum Wells, Physics and Device Applications I*, Vol. 62 of *Semiconductors and Semimetals* edited by H.C. Liu and F. Capasso, (Academic, Boston, 2000).

[8] R. Sasagawa, H. Sugawara, Y. Ohno, H. Nakajima, S. Tsujino, H. Akiyama, and H. Sakaki, Appl. Phys. Lett. **72**, 719 (1998).

[9] R.J. Warburton, K. Weilhammer, J.P. Kotthaus, M. Thomas, and H. Kroemer, Phys. Rev. Lett. **80**, 2185 (1998).

[10] S. Graf, H. Sigg, K. Köhler, and W. Bächtold, Phys. Rev. Lett. **84**, 2686 (2000).

[11] H.C. Liu, and A.J. SpringThorpe, Phys. Rev. B **61**, 15 629 (2000).

[12] S. Tsujino, M. Rufenacht, H. Nakajima, T. Noda, C. Metzner, and H. Sakaki, Phys. Rev. B **62**, 1560 (2000).

[13] S. Ernst, A.R. Goni, K. Syassen, and K. Eberl, Phys. Rev. Lett. **72**, 4029 (1994).

[14] D.F. Nelson, R.C. Miller, and D.A. Kleinman, Phys. Rev. B **35**, 7770 (1987).

[15] C. Metzner and G.H. Döhler, Phys. Rev. B **60**, 11 005 (1999).

[16] R. Duer, D. Gershoni, and E. Ehrenfreund, Superlattices Microstruct. **17**, 5 (1995).

[17] R. Duer, I. Shtrichman, D. Gershoni, and E. Ehrenfreund, Phys. Rev. Lett. **78**, 3919 (1997).

[18] I. Shtrichman, D. Gershoni, and R. Kalish, Phys. Rev. B **56**, 1509 (1997).

[19] D. Gershoni, C.H. Henry, and G.A. Baraff, IEEE J. Quantum Electron. **29**, 2433 (1993).

[20] S. Schmitt-Rink, D.S. Chemla, and D.A.B. Miller, Adv. Phys. **38**, 89 (1989).

[21] It is interesting to compare these numerical results to an analytical calculation of the individual many-body effects, in which the single-particle wave functions of the empty QW are used to evaluate the subband shifts in the framework of first-order perturbation theory (assuming only one type of carriers). For the case of a square QW with infinite barriers one obtains $|\Delta E_D(n)/\Delta E_H(n)|=16/9$ and $|\Delta E_{\mathrm{exc}}(n)/\Delta E_{\mathrm{XC}}(n)|=2$ for the ratios between the dynamic and corresponding static corrections. Remarkably, the analagous calculation for a parabolic well yields $|\Delta E_D(n)/\Delta E_H(n)|=1$ and $|\Delta E_{\mathrm{exc}}(n)/\Delta E_{\mathrm{XC}}(n)|=1$, i.e., exact cancellation of all terms. This means that (even within this simple approximation) the ISB resonance in a harmonic well is independent of the electron density, in agreement with Kohn's theorem. Note, however, that the perturbation approximation fails at higher densities, as soon as the self-consistent Hartree wave functions start to differ from the unperturbed single-particle functions.